

60 GHz Reference Chip Antenna for Gain Verification of Millimeter Wave Test Chambers

William E. McKinzie III
WEMTEC, Inc.
Fulton, MD USA
will@wemtecinc.com

Per Iversen and Edward Szpindor
Orbit/FR Inc.
Horsham, PA USA

Michael A. Smith and Bradley A. Thrasher
DuPont Microcircuit Materials
Research Triangle Park, NC USA

Abstract— We have developed a 60 GHz chip antenna designed for use as a gain and pattern verification tool in the calibration process of a millimeter wave antenna test chamber. The antenna is designed to interface with ground-signal-ground (GSG) micro-probes that have a probe pitch of 150 μm to 250 μm . This low temperature cofired ceramic (LTCC) chip antenna is fabricated using DuPont's 9K7 GreenTape™ material system with gold conductors. Features include a wafer-probe transition, a shielded stripline corporate feed network, aperture coupled patch elements, and an integrated Sievenpiper electromagnetic bandgap (EBG) structure for surface wave mode suppression. The use of the EBG structure enables main beam gain enhancement and side lobe level suppression. This 2x2 antenna array is directive such that it offers a nominal gain of 12 dBi at broadside over 58-62 GHz with an antenna efficiency of at least 60%. The entire antenna package has a nominal size of only 10.9 mm x 12.2 mm x 0.71 mm. Since this antenna package material is hermetic, it has stable performance under varying humidity and temperature which is highly desirable as a reference antenna.

I. INTRODUCTION

Millimeter wave antennas are often designed to be probed by a ground-signal-ground (GSG) micro-probe. Probe-fed antennas have a number of characterization challenges [1], [2]. Measuring their gain in an antenna test chamber or test setup requires a gain calibration process. In some cases, this means the removal of the micro-probe and the insertion of a coax-to-waveguide adapter plus a calibrated standard gain waveguide horn [3]. In another test setup a direct transmission line connection is made between the source that drives the micro-probe and the receiving mixer [4]. Each millimeter wave component removed and added in the calibration process must be carefully measured as a two-port network and the component loss included in the gain calibration calculation. One problem that arises is the uncertainty in loss associated with the physical removal and installation of every component. Coaxial connectors and waveguide flanges must be torqued to the correct specification, but even with the perfect torque, there is still uncertainty in the resulting loss of individual components. A 60 GHz antenna test setup has been estimated

to have an overall gain accuracy of ± 0.8 dB [4], [5] based on loss uncertainties. Millimeter wave gain calibration processes can also be very time consuming and quite tedious, demanding careful attention to achieve a good calibration. Therefore, it is highly desirable to have a gain standard, or at least a gain verification antenna, with a micro-probe interface.

Any reference antenna employed for gain calibration purposes needs to be stable over time, varying temperature, and varying humidity. To meet these requirements we have selected low temperature cofired ceramic (LTCC) as a stable package material. Here we introduce a reference antenna fabricated with DuPont 9K7 GreenTape™ [6], [7] and Au metal paste for interior conductive traces (DuPont LL505) and exterior conductive traces (DuPont LL507). This LTCC material is hermetic, and its relative permittivity of 7.1 varies linearly with temperature at a rate of only $7\text{E-}4$ / $^\circ\text{C}$. Split cavity resonator tests at 9.5 GHz have shown that 9K7 GreenTape is very stable lot-to-lot with a relative permittivity of 7.1 ± 0.2 in tests of more than 25 production lots. Open resonator tests have shown that 9K7 has a dielectric loss tangent of only .0015 at 60 GHz.

An important objective of a reference antenna is to reduce power radiated in the direction of the micro-probe, and therefore a directive antenna is needed. Our reference antenna is a linearly polarized 2x2 patch array with a medium level of directivity of about 13 dBi at broadside. To further achieve this objective, the propagation of TM mode surface waves is suppressed with an integrated and compact Sievenpiper electromagnetic bandgap (EBG) structure [8]-[10]. This EBG structure has been shown to enhance boresight gain in 60 GHz LTCC antennas by at least 4 dBi [11], [12] and to improve the E-plane side lobe level by about 8 dB [11], [12]. Our reference antenna employs the same EBG unit cell structure as demonstrated in [11] and [12] where its TM mode cutoff frequency of 53 GHz has been measured using EBG test vehicles as described in [13].

II. ANTENNA DESIGN AND FABRICATION

A photograph of the 60 GHz reference chip antenna is shown in Fig. 1. Fig. 2 shows orthogonal views and package

dimensions. Overall dimensions are $430 \times 480 \times 28 \text{ mil}^3$ or $10.92 \text{ mm} \times 12.19 \text{ mm} \times 0.71 \text{ mm}$. The aperture area including EBG structure is $9.4 \text{ mm} \times 10.92 \text{ mm}$, or $1.88\lambda \times 2.18\lambda$ at 60 GHz. Radiating elements have an inter-element spacing of 3.05 mm, or 0.61λ at 60 GHz in both principal planes.

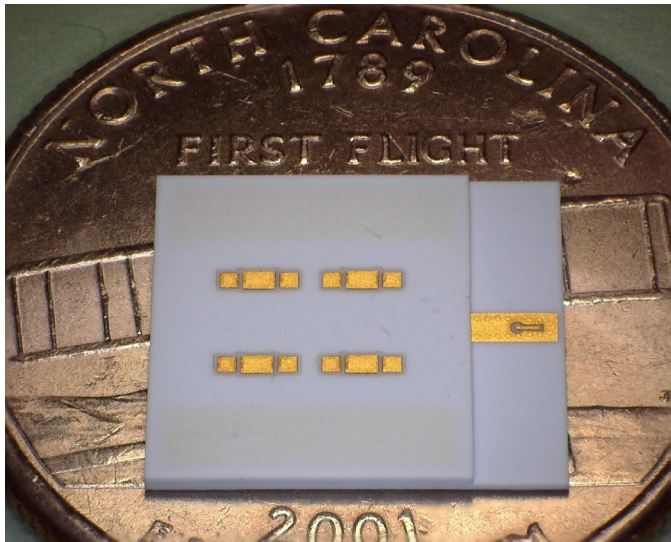


Figure 1. Photo of the 60 GHz reference chip antenna resting on a US quarter.

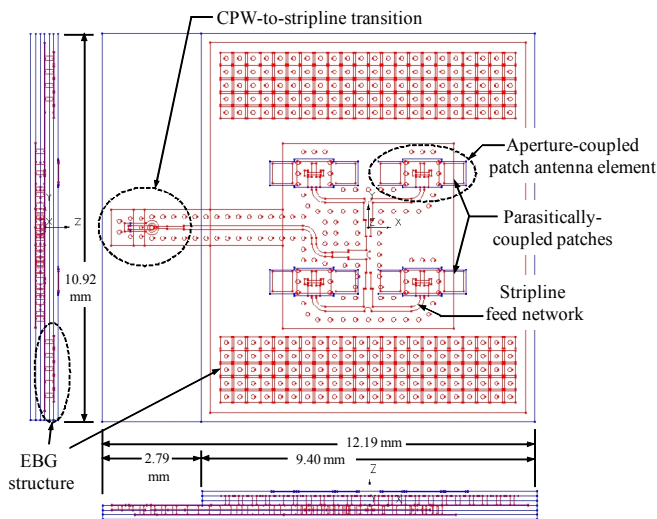


Figure 2. Orthogonal views of the reference chip antenna. Dielectric layers are blue, conductors are red.

This reference antenna is comprised of six layers of nominal 5 mil 9K7 GreenTape, and five layers of Au metal. Key features include a broadband 50- Ω coplanar waveguide (CPW)-to-stripline (SL) transition [14] fabricated in the shelf of the LTCC package, a fully shielded SL feed network, an I-shaped coupling slot for each patch element, broadband antenna elements featuring parasitically-coupled patches, and a 5-row Sievenpiper EBG structure designed to suppress TM mode surface waves launched in the E-plane (yz -plane). See Fig. 3. Since this is a linearly polarized antenna, the EBG structure is not needed in the H-plane (xz -plane) which is free of TM mode surface waves. The lowest order TE mode surface

wave, normally launched into the H-plane, is cutoff at 60 GHz because the three-layer thick LTCC substrate supporting the patch antenna elements is electrically too thin at this frequency. Note there is a common ground plane in the center of the LTCC stackup which forms the ground plane for all radiating patches, the ground plane for the EBG structures, the upper ground plane of the SL, and the coplanar ground of the CPW-to-SL transition.

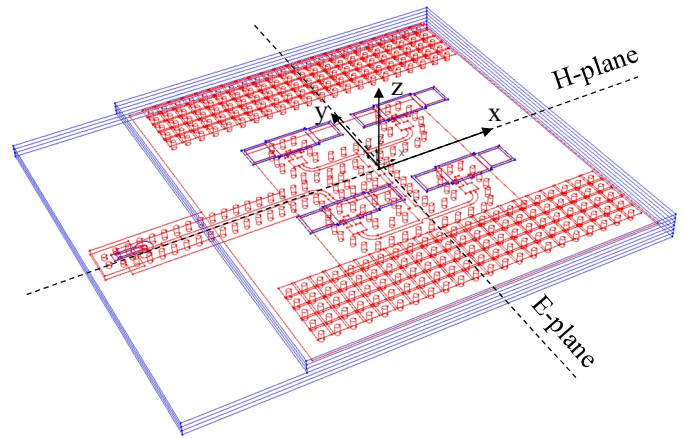


Figure 3. 3D perspective view of the reference antenna.

The SL feed network is shown below in Fig. 4 where the SL center conductor is located between tape layers 2 and 3 counting from the bottom as tape layer 1. The feed network contains three reactive power dividers to provide equal power division and equal phase to each aperture coupled patch antenna element. Each power divider has a dual stage matching network for improved bandwidth and lower loss. The entire feed network is shielded by a row of Au vias, of nominal diameter 116 μm , to suppress radiation from the SL discontinuities and from the coupling slots which excite patch elements. The nominal via pitch is either 305 μm or 356 μm .

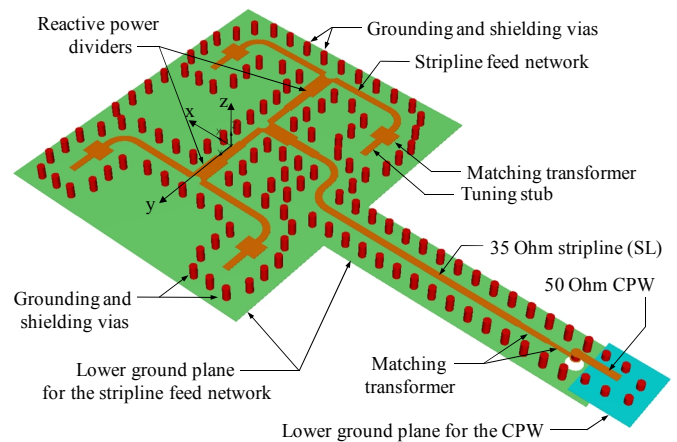


Figure 4. 3D perspective view of the shielded stripline (SL) feed network.

Full-wave simulations reveal that the more than half of the total material loss budget occurs as conductor loss in the SL center conductors of the feed network. Therefore, the characteristic impedance of the feed network has been lowered

from 50Ω to 35Ω which increases the nominal line width from $50 \mu\text{m}$ to $114 \mu\text{m}$. This change decreases the SL loss per unit length improving efficiency, and it reduces the variation in SL characteristic impedance with manufacturing tolerances. A two-stage SL matching transformer is employed at the output of the CPW-to-SL transition.

Fig. 5 shows a fabricated antenna element. The central patch is excited by an I-shaped coupling slot centered directly below it in the antenna ground plane (not shown). The two smaller parasitically-coupled patches on the left and right sides are used to increase the 10 dB return loss bandwidth up to about 8 GHz. The four patch antenna elements are each formed as a screen printed block and then laser trimmed in the post-fired state using a laser ablation process with an LPKF Protolaser [145]. Post-fired laser ablation processing yields tight tolerances of $\pm 8 \mu\text{m}$ or less for exterior metal dimensions. However, a trench remains on the exterior LTCC surface, and this trench needs to be considered in the antenna design process.

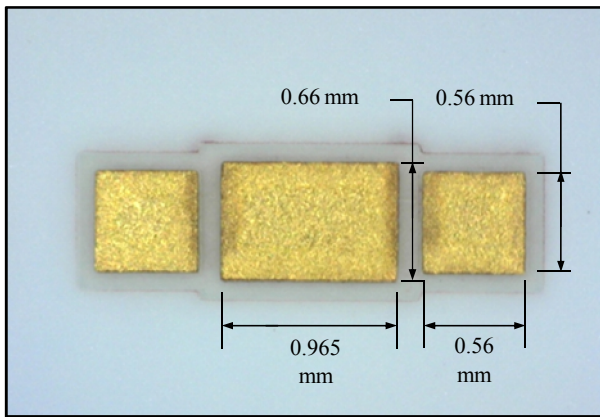


Figure 5. Each antenna element has one central driven patch and two parasitically coupled patches.

Fig. 6 shows the CPW-to-SL transition. The keyhole shaped slot is formed with post-fired laser ablation processing in external metal. The three black crosses are the nominal locations where the tips of a $200 \mu\text{m}$ GSG micro-probe should land. This reference antenna can accommodate GSG micro-probes of pitch $150 \mu\text{m}$ to $250 \mu\text{m}$. Larger probes might work but the ground tips would land on top of buried grounding vias.

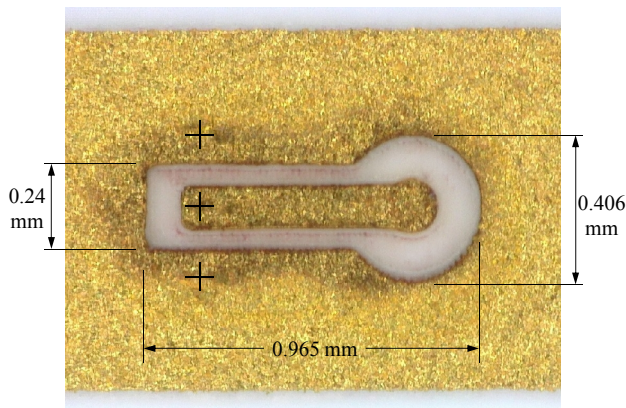


Figure 6. CPW-to-stripline transition.

III. ANTENNA PERFORMANCE

Full-wave simulation of the reference antenna was accomplished using CST Microstripes 2012. Two collinear, equal amplitude, 100Ω wire ports with opposite phase were employed to excite the slots of the CPW at the reference plane where the tips of a 50Ω micro-probe would land. Simulated and measured reflection coefficient are shown in Fig. 7. The measured data is the average of reflection coefficient from 27 antenna units of the same design. Several dozen prototype antennas were fabricated, and measurements showed very good consistency unit-to-unit for return loss, gain, and pattern shape. Both simulated and measured reflection coefficient have about 8 GHz of -10 dB bandwidth. Degradation of the measured reflection coefficient is believed to be caused by a co-fired part marking on the backside of the antenna package which created numerous short sections of lower Z_0 in the feedline where the part markings deformed the lower SL ground plane. This issue will be corrected in future builds.

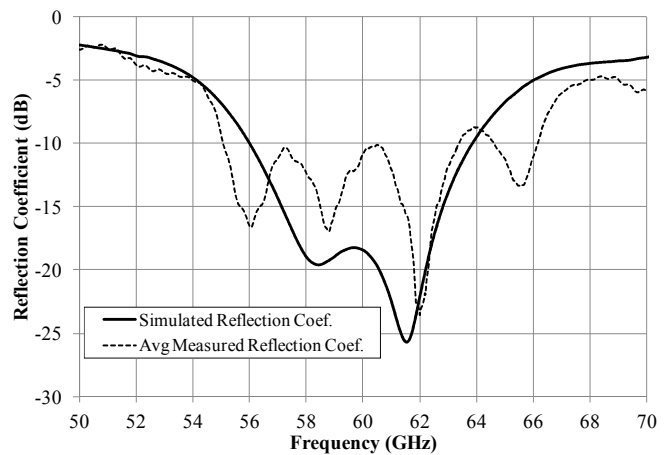


Figure 7. Comparison of simulated and measured reflection coefficient.

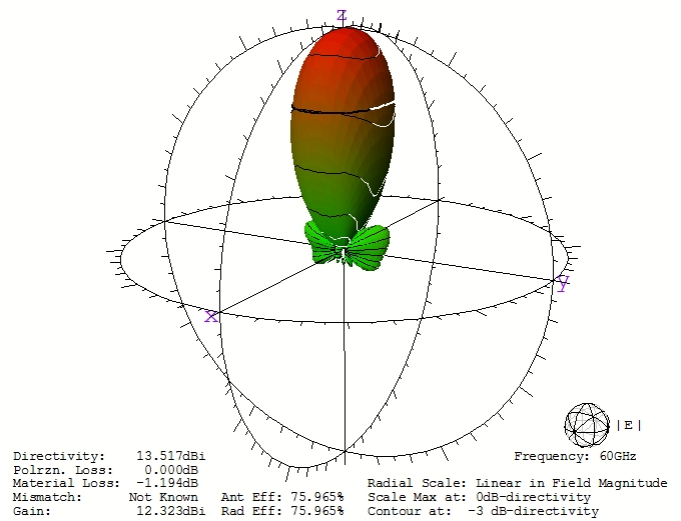


Figure 8. Simulated 3D directivity pattern at 60 GHz.

Fig. 8 above shows the simulated 3D directivity pattern where the peak directivity of 13.5 dBi is found at boresight

along the z axis. Note that the only visible side lobes on this linearly scaled 3D plot are found in the yz plane, which is the E-plane. E and H planes are illustrated in Fig. 3. Fig. 9 shows a comparison of simulated and measured E-plane gain at 60 GHz, while Fig. 10 shows this comparison for the H-plane. This measured gain is raw data which has not been modal filtered.

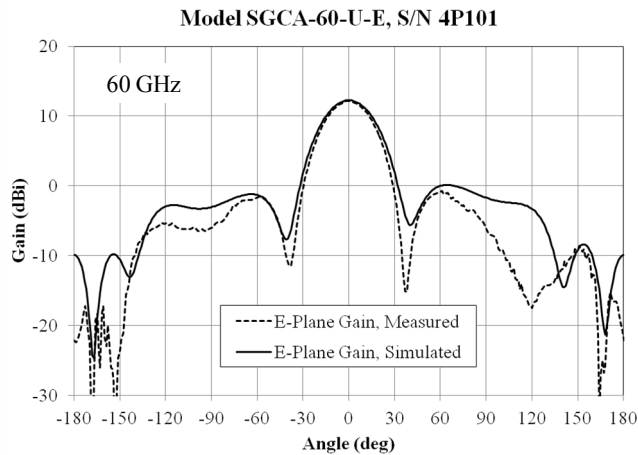


Figure 9. E-plane gain patterns; simulated and measured.

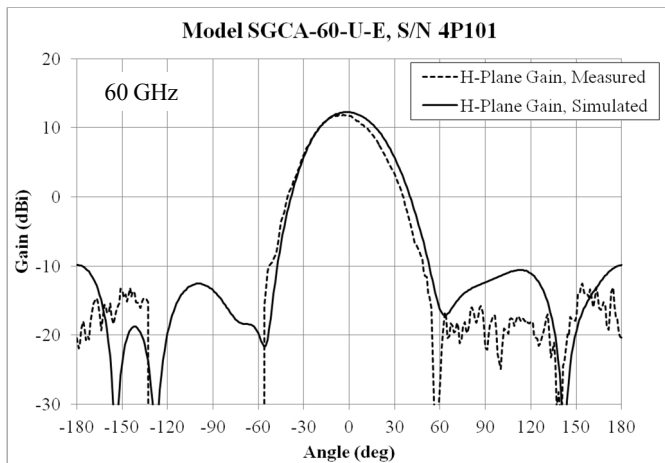


Figure 10. H-plane gain patterns; simulated and measured.

The simulated peak gain is 12.32 dBi at 60 GHz, and the measured peak gain levels agree to within +/-0.4 dB of this value for the first five prototype antennas that were measured. Antenna measurements were accomplished using a μ -Lab antenna chamber [16] and processed using MVG's 959 Spectrum™ software. It should be noted that the measured gain includes radiation and scattering from the micro-probe (Cascade ACP110-A-GSG-250) where the simulated gain is from a 3D model that does not include the micro-probe or the Rohacell foam chuck used to support the antenna under test. In spite of these differences, the main beam and side lobe levels in the upper hemisphere show good agreement between simulation and measurement. The simulated E-plane (H-plane) half-power beamwidth is 34° (42.5°). The E-plane beamwidth is narrower than the H-plane beamwidth because the inside edges of the EBG structure scatter some surface waves power which effectively increases the width of the aperture in the E-

plane. It should also be noted that the measured H-plane gain drops to a very low value between polar angles of -135° and -55° because of blockage from the micro-probe and its positioner. The simulated H-plane gain predicts a side lobe level well below -20 dB over this range of polar angles. This satisfies our objective of limiting radiation in the direction of the micro-probe and its positioner.

To investigate the pattern bandwidth of this reference antenna we plot the principal plane directivity patterns from 56 GHz to 64 GHz in 2 GHz increments. Fig. 11 shows the E-plane directivity cuts, and Fig. 12 shows the H-plane directivity patterns. The main beam shape, pointing direction, and side lobe levels are relatively stable over this frequency range.

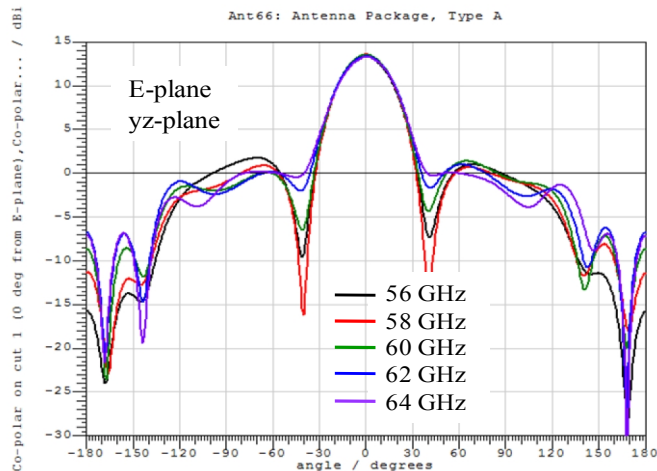


Figure 11. Simulated E-plane directivity patterns.

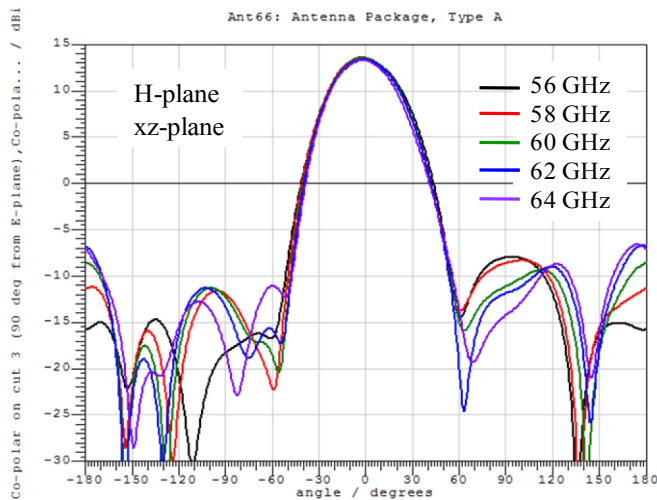


Figure 12. Simulated H-plane directivity patterns.

A swept gain plot is shown in Fig. 13. At 60 GHz, the simulated gain and measured gain are 12.32 dBi and 11.87 dBi respectively. This gain is realizable gain since it includes mismatch loss. The measured gain plot reveals that the fabricated reference antenna is tuned approximately 1.5 GHz too high in frequency. This frequency shift is believed to be caused by a laser ablated trench around the exterior patches that is wider than the simulated trench width. This issue can easily be corrected in future antenna builds by adjusting patch sizes.

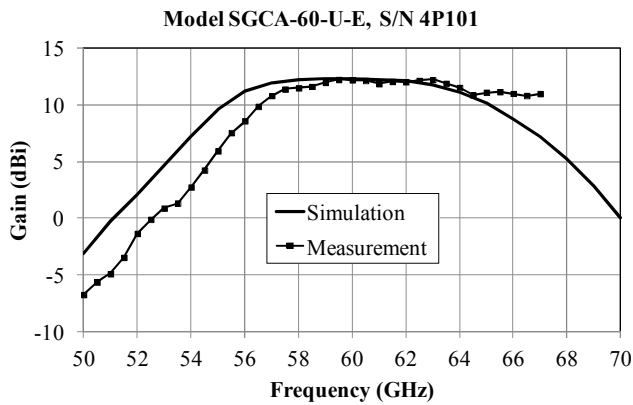


Figure 13. Swept gain; simulated and measured.

A comparison of simulated and measured antenna efficiency is shown below in Fig. 14. This antenna efficiency includes mismatch loss. At 60 GHz, the simulated and measured antenna efficiencies are approximately 74.9% and 68.4% (-1.65 dB) respectively. Measured antenna efficiency exceeds 60% (-2.22 dB) over 57-64 GHz. The simulated antenna efficiency exceeds 60% over 56-64 GHz. In future builds, with improved return loss, we expect the antenna efficiency to exceed 70% (-1.55 dB) at 60 GHz. A reference chip antenna needs to have high antenna efficiency for a variety of reasons, but one of the most obvious reasons is ensure a consistent and predictable gain level unit-to-unit.

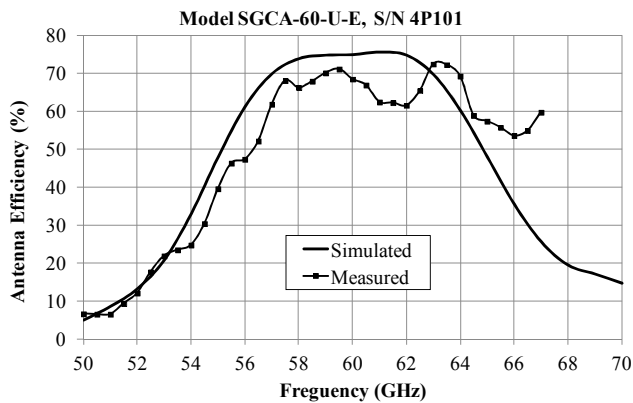


Figure 14. Antenna efficiency; simulated and measured.

IV. CONCLUSIONS

We report on a 60 GHz, LTCC, chip antenna that offers a nominal gain of 12 dBi at broadside over 58-62 GHz with an antenna efficiency of at least 60%. The entire antenna package has a nominal size of only 10.9 mm x 12.2 mm x 0.71 mm. It is designed to accommodate 50Ω GSG micro-probes of pitch 150 μm to 250 μm. This reference antenna was fabricated from DuPont 9K7 GreenTape LTCC material using Au metallization to form a hermetic package that is stable with respect to changes in humidity and temperature. To the author's knowledge, this is the first commercially available millimeter wave reference antenna designed to be fed with a GSG micro-probe. It is intended for use as a gain calibration or verification

antenna in the calibration process of a millimeter wave test chamber.

REFERENCES

- [1] A. Shamim, "Co-design of on-chip antennas and RF circuits for system-on-chip applications," Short course no. 4, *Proc. IEEE Intl. Microwave Symp.*, June 2-7, 2013, Seattle, WA. pp. 52.
- [2] E. Szpindor, W. Zhang, and P. Iverson, "Measurement uncertainties in millimeter wave on-chip antenna tests," *38th Annual Meeting and Symposium of the Antenna Measurement Techniques Association.*, Oct 30-Nov 4 2016, in-press.
- [3] B. Klein, M. Jennings, P. Seiler, K. Wolf, and D. Plettemeier, "Verification and demonstration up to 67 GHz of an on-chip antenna pattern measurement setup," *IEEE Conf. on Antenna Measurements and Applications (CAMA)*, Nov 16-19, 2014 Juan-les-Pins, Antibes, France, pp. 1-4.
- [4] D. Titz, M. Kyro, F. Ferrero, S. Ranvier, C. Luxey, P. Brachat, G. Jacquemod, and P. Vainikainen, "Measurement setup and associated calibration methodology for 3D radiation pattern of probe-fed millimeter-wave antennas," *2011 IEEE Loughborough Antennas & Propagation Conference*, Nov 14-15, Loughborough, UK, pp. 1-5.
- [5] D. Titz, F. Ferrero, and C. Luxey, "Development of a millimeter-wave measurement setup and dedicated techniques to characterize the matching and radiation performance of probe-fed antennas," *IEEE Antennas and Propagation Magazine*, vol. 54, No. 4, August 2012, pp. 188-203.
- [6] D. M. Nair, K. Souders, J. Parisi, M. Combs, and K. M. Nair, "Characterization of DuPont 9K7 LTCC Material System for Microwave Packaging Applications," *IMAPS Advanced Technology Workshop on RF and Microwave Packaging*, San Diego, CA, USA Sept. 2009
- [7] DuPont, "DuPont GreenTape Design and Layout Guidelines" [Online]. Available: http://www.dupont.com/content/dam/dupont/products-and-services/electronic-and-electrical-materials/documents/prodlib/GreenTape_Design_Layout_Guidelines.pdf
- [8] Daniel F. Sievenpiper, "High-impedance electromagnetic surfaces", Ph.D. Diss., Dept. of Electrical Engineering, University of California, Los Angeles, 1999.
- [9] Dan Sievenpiper, Lijun Zhang, Romulo F. Jimenez Broas, Nicholas G. Alexopoulos, and Eli Yablonovitch, "High-impedance electromagnetic surfaces with a forbidden frequency band," *IEEE Trans. Microwave Theory and Techniques*, Vol. 47, No. 11, November 1999.
- [10] E. Yablonovitch and D. Sievenpiper, "Circuit and method for eliminating surface currents on metals," US Patent 6,262,495 issued on July 17, 2001.
- [11] W. E. McKinzie III, D. M. Nair, B. A. Thrasher, M. A. Smith, E. D. Hughes, and J. M. Parisi, "60 GHz patch antenna in LTCC with an integrated EBG structure for antenna pattern improvements," *IEEE Antennas and Propagation Society Intl. Symp.*, Memphis, TN, July 6-11, 2014, pp. 1766-1767.
- [12] W. E. McKinzie III, D. M. Nair, B. A. Thrasher, M. A. Smith, E. D. Hughes, and J. M. Parisi, "60 GHz 2x2 LTCC patch array with an integrated EBG structure for gain enhancement," *IEEE Antennas and Wireless Propagation Lett.*, Vol. 15, 2016, pp. 1522-1525.
- [13] W. E. McKinzie III, D. M. Nair, B. A. Thrasher, M. A. Smith, E. D. Hughes, and J. M. Parisi, "Millimeter Wave Measurement of the TM Mode Cutoff for EBG Structures Fabricated in LTCC for Antenna Applications," *2013 IEEE Antennas and Propagation Intl. Symp.*, Lake Buena Vista, FL, July 5-12, 2013, pp. 83-84.
- [14] D. M. Nair, W. E. McKinzie III, B. A. Thrasher, M. A. Smith, E. D. Hughes, and J. M. Parisi, "A 10 MHz to 100 GHz LTCC CPW-to-stripline vertical transition," *Proc. IEEE Intl. Microwave Symp.*, Seattle, WA, USA, June 2-7, 2013, pp. 1-4.
- [15] <http://www.lpkf.com/products/rapid-pcb-prototyping/laser-circuit-structuring/micromaterial-processing-protolaser-u4.htm>
- [16] http://www.mvg-world.com/products/field_product_family/antenna-measurement-2/u-lab